

Research Article

Node-based differential network analysis in genomics

Xiao-Fei Zhang^{a,c}, Le Ou-Yang^{b,*}, Hong Yan^c^a School of Mathematics and Statistics & Hubei Key Laboratory of Mathematical Sciences, Central China Normal University, Wuhan, China^b College of Information Engineering, Shenzhen University, Shenzhen, 518060, China^c Department of Electronic Engineering, City University of Hong Kong, Hong Kong, China

ARTICLE INFO

Article history:

Received 24 March 2017

Accepted 27 March 2017

Available online 4 April 2017

Keywords:

Differential network analysis

Gaussian graphical model

Gene dependency network

Hub nodes

Graphical lasso

ABSTRACT

Gene dependency networks often undergo changes in response to different conditions. Understanding how these networks change across two conditions is an important task in genomics research. Most previous differential network analysis approaches assume that the difference between two condition-specific networks is driven by individual edges. Thus, they may fail in detecting key players which might represent important genes whose mutations drive the change of network. In this work, we develop a node-based differential network analysis (N-DNA) model to directly estimate the differential network that is driven by certain hub nodes. We model each condition-specific gene network as a precision matrix and the differential network as the difference between two precision matrices. Then we formulate a convex optimization problem to infer the differential network by combining a D-trace loss function and a row-column overlap norm penalty function. Simulation studies demonstrate that N-DNA provides more accurate estimate of the differential network than previous competing approaches. We apply N-DNA to ovarian cancer and breast cancer gene expression data. The model rediscovers known cancer-related genes and contains interesting predictions.

© 2017 Elsevier Ltd. All rights reserved.

1. Introduction

A key challenge in genomic research is to characterize complex interactions of molecular entities such as genes and their products (Barabási et al., 2011; Zhang et al., 2015a). Genes within cell signaling pathways interact with each other to form networks that regulate various cellular functions. It is well-established that a gene dependency network can undergo change in response to different conditions such as DNA damage or environmental stress (de la Fuente, 2010; Ideker and Krogan, 2012; Ou-Yang et al., 2014; Grechkin et al., 2016; Zhang et al., 2016a). Thus, it is of great interest to explore how the gene network changes between two conditions. Indeed, differential network analysis has become an important tool in bioinformatics which is complement to differential expression analysis (de la Fuente, 2010; Gill et al., 2010; Ha et al., 2015).

Gene networks are often modeled as Gaussian graphical models (Friedman, 2004; Markowetz and Spang, 2007). These models assume that the gene expression levels are generated from a multivariate Gaussian distribution (Cox and Wermuth, 1996). As a consequence, the conditional dependencies between genes

can be determined directly from nonzero elements of the precision matrix (or inverse covariance matrix) (Lauritzen, 1996), where two genes are conditionally independent given the other genes if and only if the corresponding element of the precision matrix is zero. Therefore, the condition-specific gene networks can be modeled as the corresponding precision matrices (Yuan and Lin, 2007; Friedman et al., 2008; Rothman et al., 2008). Then, the different network between two conditions can be modeled as the difference between the two condition-specific precision matrices (Danaher et al., 2014; Mohan et al., 2014; Zhao et al., 2014; Huang and Chen, 2015; Yuan et al., 2015a; Zhang et al., 2016b).

There are two main types of approaches to estimate the differential network based on Gaussian graphical models. The most straightforward one is to estimate the condition-specific precision matrices first and then subtract the estimates (Ha et al., 2015; Danaher et al., 2014; Mohan et al., 2014; Zhang et al., 2016b). The inverse of the sample covariance matrix can be a naive estimate of a single precision matrix. However, when the number of genes exceeds the number of subjects, the sample covariance matrix is not invertible. Based on the prior knowledge that many pairs of genes are conditionally independent, graphical lasso models (Yuan and Lin, 2007; Friedman et al., 2008; Rothman et al., 2008) have been proposed to obtain sparse estimate of the precision matrix. The

* Corresponding author.

E-mail address: szuouyl@gmail.com (L. Ou-Yang).

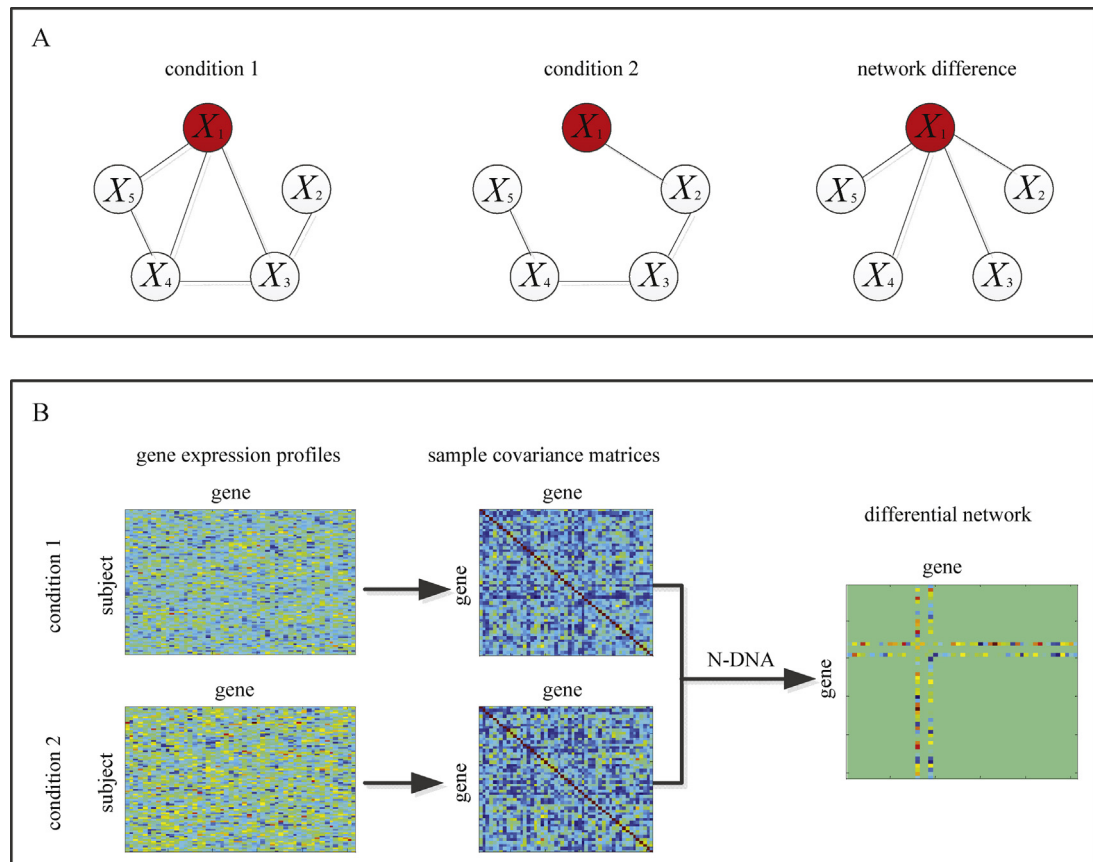


Fig. 1. Motivation and overview of our work. (A) A toy example that illustrates the change of a network of 5 genes between two different conditions. The perturbation of network might be due to a driver mutation on gene X_1 that alters its regulatory interactions with the other four genes. Gene X_1 might represent a key regulator (e.g., transcription factor) that is mutated or abnormally expressed in one condition, in turn changing the underlying gene network. Therefore, the differential network might be driven by certain hub genes. (B) An overview of our method. The input data are two condition-specific gene expression data. Then the condition-specific sample covariance matrices are computed. Based on the estimated sample covariance matrices, we directly estimate the differential network using the proposed N-DNA model. Our N-DNA does not require to estimate the individual gene networks and can impose hub structure on the resulting differential network.

standard graphical lasso models separately estimate the condition-specific precision matrices using subjects within each condition. They might be suboptimal when there exist common structures shared by different conditions (Danaher et al., 2014; Ha et al., 2015; Mohan et al., 2014). To deal with this problem, several joint estimation approaches have been proposed by employing various group penalties (Danaher et al., 2014; Ha et al., 2015; Mohan et al., 2014; Huang and Chen, 2015; Guo et al., 2011; Lee and Liu, 2015; Zhang et al., 2016b). Most of these approaches assume that the individual precision matrices are sparse. However, the sparsity assumption can be violated if the gene network contains hub nodes which connect with many other nodes (Zhao et al., 2014). In addition, their power in detecting weak interactions is limited since the corresponding elements in precision matrices might be shrunk toward zero. There are many interactions whose strengths are weak in single condition but their changes between two conditions are large. Simply subtracting two estimated precision matrices would overlook these changes (Yuan et al., 2015a).

The second type of approach is to directly estimate the difference between the condition-specific precision matrices. Zhao et al. (2014) proposed a differential network analysis approach which does not require the individual precision matrices to be sparse. Their approach outperforms fused graphical lasso (Danaher et al., 2014) when the individual networks include hubs. However, their approach is computationally prohibitive when the number of genes is large. Based on the D-trace loss function which is developed to estimate precision matrix (Zhang and Zou, 2014), Yuan et al.

(2015a) developed a new loss function to directly estimate the differential network, which can be solved more efficiently than the loss function used by Zhao et al. (2014). Tian et al. (2016) also proposed a direct estimation method that is similar to (Yuan et al., 2015a) but use a different algorithm to solve the model. All the three approaches apply a lasso penalty to each edge, which means each edge is treated equally and independent of the others (Mohan et al., 2014; Tan et al., 2014). This is unrealistic in many real-world applications, where there might exist certain hub nodes in the differential network that represent the perturbed regulator genes. Even though the three direct estimation approaches allow the presence of hub nodes in each condition-specific network, they are not designed for encouraging the appearance of hub nodes in the differential network.

In this paper, we estimate the differential network between two conditions, which is driven by certain perturbed regulatory genes. By combining the D-trace loss function (Yuan et al., 2015a) and the row-column overlap norm regularizer (Mohan et al., 2014), we develop a node-based differential network analysis (N-DNA)

model that estimates the differential network directly and does not require to estimate individual condition-specific networks. We also propose an alternating direction method of multiplier (ADMM) algorithm to solve the optimization problem. In simulation studies, we observe that D-NDA recovers the differential network more accurately than previous competing approaches. To evaluate the performance of D-NDA on real biological data, we apply it to the challenging problem of identifying the differential network associated with platinum resistance in ovarian cancer and the differential network between tumor tissue and normal tissue in breast cancer. We identify two key regulator genes (IRS1 and PDPK1) for ovarian cancer and three perturbed genes (KIT, NOTCH1 and SHC4) for breast cancer. According to previous literature, we find that the five genes play an important role in cancer.

2. Methods

2.1. Problem formalization and notations

Suppose that we have independent observations of p genes from two groups of subjects: $X_i = (X_{i1}, \dots, X_{ip})^T$ for $i = 1, \dots, n_X$ from one group and $Y_i = (Y_{i1}, \dots, Y_{ip})^T$ for $i = 1, \dots, n_Y$ from the other group. The two groups can correspond to two distinct conditions. Furthermore, we assume that the covariance matrices for the two groups are Σ_X and Σ_Y , respectively. The differential network is defined to be the difference between the two condition-specific precision matrices, $\Delta = \Sigma_Y^{-1} - \Sigma_X^{-1}$ (Zhao et al., 2014; Yuan et al., 2015a). The goal of this study is to estimate Δ given the two groups of observations (Fig. 1B).

For a matrix $A \in R^{p \times p}$ with element A_{ij} , $\|A\|_1 = \sum_{j=1}^p \sum_{k=1}^p |A_{jk}|$ will denote the elementwise L_1 norm, $\|A\|_\infty = \max_{j,k} |A_{jk}|$ will denote the elementwise maximum norm, $\|A\|_F = \sqrt{\sum_{j=1}^p \sum_{k=1}^p A_{jk}^2}$ will denote the Frobenius norm, and $\|A\|_{2,1} = \sum_{k=1}^p \|A_k\|_2 = \sum_{k=1}^p \sqrt{\sum_{j=1}^p A_{jk}^2}$ will denote the $L_{2,1}$ norm, where A_k denotes the k -th column of A .

2.2. Node-based differential network analysis model

Let $\hat{\Sigma}_X = \frac{1}{n_X} \sum_{i=1}^{n_X} (X_i - \hat{\mu}_X)(X_i - \hat{\mu}_X)^T$ be the sample covariance matrix for the first group, where $\hat{\mu}_X = \frac{1}{n_X} \sum_{i=1}^{n_X} X_i$. We define $\hat{\Sigma}_Y$ similarly for the other group. To obtain a symmetric matrix $\Delta = \Sigma_Y^{-1} - \Sigma_X^{-1}$ which represents the differential network between the two groups, we consider the D-trace loss function which is introduced in (Yuan et al., 2015a):

$$L_D(\Delta, \hat{\Sigma}_X, \hat{\Sigma}_Y) = \frac{1}{2} \langle \Delta^2, (\hat{\Sigma}_X \hat{\Sigma}_Y + \hat{\Sigma}_Y \hat{\Sigma}_X) / 2 \rangle - \langle \Delta, \hat{\Sigma}_X - \hat{\Sigma}_Y \rangle. \quad (1)$$

Yuan et al. (2015a) have proved that $L_D(\Delta, \hat{\Sigma}_X, \hat{\Sigma}_Y)$ is convex with respect to Δ if $\hat{\Sigma}_X$ and $\hat{\Sigma}_Y$ are positive definite and the unique minimizer of (1) is achieved at $\hat{\Sigma}_Y^{-1} - \hat{\Sigma}_X^{-1}$. Thus, we can obtain an estimate of Δ by minimizing $L_D(\Delta, \hat{\Sigma}_X, \hat{\Sigma}_Y)$.

Based on the assumption that the differential network is driven by certain genes whose connectivity patterns to other nodes are completely changed between the two conditions (Mohan et al., 2014; Grechkin et al., 2016), we use the row-column overlap norm penalty (Mohan et al., 2014; Tan et al., 2014) to detect the differential network that contains hub nodes:

$$P(\Delta) = \min_{\Delta, V: \Delta = V + V^T} \lambda_1 \|V\|_1 + \lambda_2 \sum_{k=1}^p \|V_k\|_2. \quad (2)$$

Here λ_1 and λ_2 are nonnegative tuning parameters. $P(\Delta)$ is a convex penalty that decomposes the estimate as $\Delta = V + V^T$, where V is a matrix whose columns are either entirely zero or almost entirely non-zero (Tan et al., 2014), where non-zero columns of V correspond to hub nodes. λ_1 controls the sparsity of each hub node's connections to other nodes, and λ_2 controls the selection of hub nodes. For details, refer to (Mohan et al., 2014; Tan et al., 2014). The parameter selection strategy is presented in Section 2.4.

By combining the D-trace loss function (1) and the hub penalty function (2), we develop a node-based differential network analysis (N-DNA) model:

$$\begin{aligned} \min_{\Delta = \Delta^T, V} \quad & L_D(\Delta, \hat{\Sigma}_X, \hat{\Sigma}_Y) + \lambda_1 \|V\|_1 + \lambda_2 \sum_{k=1}^p \|V_k\|_2 \\ \text{subject to} \quad & \Delta = V + V^T. \end{aligned} \quad (3)$$

Since both the loss function and the penalty function are convex, the proposed N-DNA model is also convex. Unlike previous direct estimate approaches (Zhao et al., 2014; Yuan et al., 2015a; Tian et al., 2016), our model is developed for estimating differential network that is driven by mutations of certain regulator genes. Compared to perturbed-node joint graphical lasso (PNJGL) (Mohan et al., 2014) which jointly estimates condition-specific precision matrices, N-DNA has two advantages: (1) N-DNA can be solved more efficiently thanks to the use of the D-trace loss function; (2) N-DNA is more powerful in detect interactions which are weak in a single condition but strong in the change of conditions, since N-DNA estimates the differential network directly and does not impose a lasso-type penalty on individual precision matrices.

2.3. Algorithm

We derive an alternating direction method of multipliers (ADMM) algorithm (Boyd et al., 2011) for the optimization problem (3). For a brief review of ADMM algorithms, please refer to (Mohan et al., 2014; Zhang et al., 2016b). We introduce a new optimization variable W and rewrite (3) as follows:

$$\begin{aligned} \min_{\Delta = \Delta^T, V, W} \quad & L_D(\Delta, \hat{\Sigma}_X, \hat{\Sigma}_Y) + \lambda_1 \|V\|_1 + \lambda_2 \sum_{k=1}^p \|V_k\|_2 \\ \text{subject to} \quad & \Delta = V + W, \quad V = W^T. \end{aligned} \quad (4)$$

The augmented Lagrangian to (4) is given by

$$\begin{aligned} L_\rho(\Delta, V, W, P, Q) = & L_D(\Delta, \hat{\Sigma}_X, \hat{\Sigma}_Y) + \lambda_1 \|V\|_1 \\ & + \lambda_2 \sum_{k=1}^p \|V_k\|_2 + \langle P, \Delta - (V + W) \rangle + \langle Q, V - W^T \rangle \\ & + \frac{\rho}{2} \|\Delta - (V + W)\|_F^2 + \frac{\rho}{2} \|V - W^T\|_F^2, \end{aligned} \quad (5)$$

where P and Q are Lagrange multipliers and serve as dual variables, and $\rho > 0$ is a penalty parameter.

In each iteration of the ADMM algorithm, each primal variable (Δ , V or W) is updated in turn by minimizing the augmented Lagrangian (5) while the other variables are fixed and then the dual variables (P and Q) are updated using a dual-ascent update rule. Below, we present the update rules for the primal variables.

Updating Δ . To update Δ with the other variables fixed, the optimization problem (5) is formulated as follows

$$\begin{aligned}\Delta &= \operatorname{argmin}_{\Delta=\Delta^T} L_\rho(\Delta, V, W, P, Q) \\ &= \operatorname{argmin}_{\Delta=\Delta^T} \frac{1}{2} \langle \Delta^2, (\hat{\Sigma}_X \hat{\Sigma}_Y + \hat{\Sigma}_Y \hat{\Sigma}_X) / 2 + \rho I \rangle \\ &\quad - \langle \Delta, \hat{\Sigma}_X - \hat{\Sigma}_Y + \rho(V + W) - P \rangle.\end{aligned}\quad (6)$$

For p -dimensional positive-definite matrix A and p -dimensional symmetric matrix B , we consider the operator $G(A, B)$ (Zhang and Zou, 2014):

$$\begin{aligned}G(A, B) &= \operatorname{argmin}_{\Delta=\Delta^T} \left\{ \frac{1}{2} \langle \Delta^2, A \rangle - \langle \Delta, B \rangle \right\} \\ &= U_A \left\{ (U_A^T B U_A) \circ C \right\} U_A^T,\end{aligned}\quad (7)$$

where $U_A D U_A^T$ is the eigenvalue decomposition of A , with ordered eigenvalues $d_1 \geq \dots \geq d_p$, \circ denotes the Hadamard product of matrices, and $C_{ij} = 2 / (d_i + d_j)$. Now (6) follows the definition of the operator $G(A, B)$ that

$$\Delta = G \left\{ (\hat{\Sigma}_X \hat{\Sigma}_Y + \hat{\Sigma}_Y \hat{\Sigma}_X) / 2 + \rho I, \hat{\Sigma}_X - \hat{\Sigma}_Y + \rho(V + W) - P \right\}. \quad (8)$$

Updating V . To update V , from (5) we have

$$\begin{aligned}V &= \operatorname{argmin}_V L_\rho(\Delta, V, W, P, Q) \\ &= \operatorname{argmin}_V \frac{1}{2} \left\| V - \frac{1}{2} \left((\Delta - W + W^T) + \frac{1}{\rho} (P - Q) \right) \right\|_F^2 \\ &\quad + \frac{\lambda_1}{2\rho} \|V\|_1 + \frac{\lambda_2}{2\rho} \sum_{k=1}^p \|V_k\|_2.\end{aligned}\quad (9)$$

For simplicity, we denote $H = \frac{1}{2} (\Delta - W + W^T) + \frac{1}{2\rho} (P - Q)$. Problem (9) is a sparse group lasso problem which has closed form solution (Friedman et al., 2010; Danaher et al., 2014; Mohan et al., 2014):

$$V_k = \max \left\{ 1 - \frac{\lambda_2}{2\rho \|S(H_k, \frac{\lambda_1}{2\rho})\|_2}, 0 \right\} \cdot S \left(H_k, \frac{\lambda_1}{2\rho} \right) \quad (10)$$

for $k=1, \dots, p$. Here $S(h, \lambda)$ denotes the soft-thresholding operator (Parikh and Boyd, 2014), applied element-wise to a vector: $S(h_j, \lambda) = \operatorname{sign}(h_j) \max(|h_j| - \lambda, 0)$.

Updating W . To update W , we have

$$\begin{aligned}W &= \operatorname{argmin}_W L_\rho(\Delta, V, W, P, Q) \\ &= \operatorname{argmin}_W \rho \left\| W - \frac{1}{2} \left((\Delta - V + V^T) + \frac{1}{\rho} (P + Q^T) \right) \right\|_F^2 \\ &= \frac{1}{2} (\Delta - V + V^T) + \frac{1}{2\rho} (P + Q^T).\end{aligned}\quad (11)$$

Based on the analysis above, we summarize the complete ADMM algorithm for the N-DNA model (3) in Algorithm 1. This algorithm can be accelerated by adaptively changing ρ (Lin et al., 2010). We set $\rho=0.1$ and increase it in the next iteration as $\rho \cdot \rho^{\text{incr}}$, and we set $\rho^{\text{incr}} = 1.05$ in our algorithm. In the implementation of the algorithm, the convergence condition is

$$\|\Delta^{t+1} - \Delta^t\|_F \leq \epsilon \|\Delta^t\|_F, \quad (12)$$

where Δ^t denotes the estimate of Δ in the t th iteration, and ϵ is a tolerance which is chosen in our experiments to equal 10^{-4} .

Algorithm 1. ADMM algorithm for the node-based differential network analysis (N-DNA) model (3)

• **Inputs:** Sample covariance matrices $\hat{\Sigma}_X$ and $\hat{\Sigma}_Y$, parameters λ_1 and λ_2 .
• **Output:** Estimated differential network $\hat{\Delta}$.

- 1: Initialize: Primal variables (Δ, V and W) to be identity matrix and dual variables to be zero matrix, $\rho=0.1$, $\rho^{\text{incr}}=1.05$, $\rho^{\text{max}}=10^{10}$.
- 2: **while** not converged **do**
- 3: $\Delta \leftarrow G \left\{ (\hat{\Sigma}_X \hat{\Sigma}_Y + \hat{\Sigma}_Y \hat{\Sigma}_X) / 2 + \rho I, \hat{\Sigma}_X - \hat{\Sigma}_Y + \rho(V + W) - P \right\}$;
- 4: $H \leftarrow \frac{1}{2} (\Delta - W + W^T) + \frac{1}{2\rho} (P - Q)$;
- 5: $V_k \leftarrow \max \left\{ 1 - \frac{\lambda_2}{2\rho \|S(H_k, \frac{\lambda_1}{2\rho})\|_2}, 0 \right\} \cdot S \left(H_k, \frac{\lambda_1}{2\rho} \right)$ for $k=1, \dots, p$;
- 6: $W \leftarrow \frac{1}{2} (\Delta - V + V^T) + \frac{1}{2\rho} (P + Q^T)$;
- 7: $P \leftarrow P + \rho (\Delta - (V + W^T))$;
- 8: $Q \leftarrow Q + \rho (V - W^T)$;
- 9: $\rho \leftarrow \min(\rho \cdot \rho^{\text{incr}}, \rho^{\text{max}})$;
- 10: Check the convergence condition.
- 11: **end while**
- 12: **return** $\hat{\Delta} = V + V^T$.

2.4. Tuning parameter selection

For N-DNA, the tuning parameter λ_1 controls the sparsity of each hub node's connections to other nodes. Large values of λ_1 tend to yield hub nodes with small degrees and small values of λ_1 yield hub nodes with large degrees. The tuning parameter λ_2 controls the selection of hub nodes. When λ_2 is larger, fewer hub nodes will be detected. Therefore, the choice of λ_1 and λ_2 is critical. However, tuning parameter selection in graphical models remains an open problem. Existing approaches such as Akaike information criterion, Bayesian information criterion, cross-validation and stability selection have been used in previous studies. Since the three approaches (Zhao et al., 2014; Yuan et al., 2015a; Tan et al., 2014) which are similar to our approach use the Akaike information criterion, we propose an Akaike Information Criterion (AIC)-type quantity for tuning parameter selection in (3):

$$\begin{aligned}AIC(\lambda_1, \lambda_2) &= (n_X + n_Y) \left\| (\hat{\Sigma}_X \hat{\Delta}_{\lambda_1, \lambda_2} \hat{\Sigma}_Y + \hat{\Sigma}_Y \hat{\Delta}_{\lambda_1, \lambda_2} \hat{\Sigma}_X) / 2 - \hat{\Sigma}_X + \hat{\Sigma}_Y \right\|_\infty \\ &\quad + 2 \cdot (v_{\lambda_1, \lambda_2} + c \cdot (|\hat{V}_{\lambda_1, \lambda_2}| - v_{\lambda_1, \lambda_2})),\end{aligned}\quad (13)$$

where $\hat{\Delta}_{\lambda_1, \lambda_2}$ and $\hat{V}_{\lambda_1, \lambda_2}$ are estimators of parameters based on tuning parameters λ_1 and λ_2 , $v_{\lambda_1, \lambda_2} = \sum_{k=1}^p I \{ \|\hat{V}_{\lambda_1, \lambda_2, k}\|_0 > 0 \}$ is the number of detected hub nodes, $|\hat{V}_{\lambda_1, \lambda_2}|$ denotes the number of nonzero elements in $\hat{V}_{\lambda_1, \lambda_2}$, and c is a constant between zero and one. The first term is the loss function which is used in Zhao et al. (2014). The second term is twice of the degrees of freedom, where the degrees of freedom is defined in a similar way to Tan et al. (2014). One can choose the values of λ_1 and λ_2 for which the quantity $AIC(\lambda_1, \lambda_2)$ is minimized. In this study, we set $c=0.2$ as suggested by Tan et al. (2014).

3. Results

In this section, we first perform simulation experiments to assess the performance of N-DNA and compare it with other Gaussian graphical model-based approaches. Then we apply N-DNA to ovarian cancer and breast cancer gene expression data.

3.1. Simulation studies

3.1.1. Data generation

In the simulation study, we consider scale-free networks because many biological networks have been reported to be scale-free and power-law degree distributions are more difficult to estimate than other simpler structure (Peng et al., 2012). We set $p=100$ genes and $n_X=n_Y=25, 50, 100$. Four of the 100 genes are

generated as hub nodes in the differential network. In detail, we generate the data as follows:

- Step 1:** We use the SFNG function in Matlab with parameters $m_{links}=2$ and $seed=1$ to generate a scale-free network with $p=100$ nodes.
- Step 2:** We create a $p \times p$ symmetric matrix A with zeros on elements not corresponding to network edges, and values from $\text{Unif}([-0.6, -0.3] \cup [0.3, 0.6])$ on elements corresponding to network edges.
- Step 3:** We duplicate A into two matrices, A_1 and A_2 . We select four nodes at random. Then, for each selected node, we randomly selected 50 elements of corresponding row and column of either A_1 or A_2 (chosen at random) and reset their values to be draws from the uniform distribution $\text{Unif}([-0.6, -0.3] \cup [0.3, 0.6])$. This results in four hub nodes with degree 50 in the differential network.
- Step 4:** We let $d = \min(\lambda_{\min}(A_1), \lambda_{\min}(A_2))$, where $\lambda_{\min}(\cdot)$ denotes the smallest eigenvalue of the matrix. To ensure positive definiteness, we set $\Sigma_X^{-1} = A_1 + (0.1 + |d|)I$ and $\Sigma_Y^{-1} = A_2 + (0.1 + |d|)I$.
- Step 5:** We generate n_X independent observations from $N(0, \Sigma_X)$ distribution and n_Y independent observations from $N(0, \Sigma_Y)$ distribution, and use them as gene expression data sets X_1, \dots, X_{n_X} and Y_1, \dots, Y_{n_Y} . Then the sample covariance matrices $\hat{\Sigma}_X$ and $\hat{\Sigma}_Y$ are computed using the generated data.

3.1.2. Simulation results

Following previous studies (Zhao et al., 2014; Yuan et al., 2015a), we use the receiver operating characteristic (ROC) curve to evaluate algorithm performance. Let $\hat{\delta}_{jk}$ be the (j, k) th entry of a given estimator $\hat{\Delta}$, and let δ_{jk} be the (j, k) th entry of the true Δ , the true positive rate (TPR) and false positive rate (FPR) are defined as

$$TPR = \frac{\sum_{j < k} I(\hat{\delta}_{jk} \neq 0 \text{ and } \delta_{jk} \neq 0)}{\sum_{j < k} I(\delta_{jk} \neq 0)},$$

$$FPR = \frac{\sum_{j < k} I(\hat{\delta}_{jk} \neq 0 \text{ and } \delta_{jk} = 0)}{\sum_{j < k} I(\delta_{jk} = 0)}.$$

We compare the performance of N-DNA to D-trace loss estimate (Yuan et al., 2015a), latent differential graphical model (LDGM) (Tian et al., 2016) and perturbed-node joint graphical lasso (PNJGL) (Mohan et al., 2014). D-trace loss estimate and LDGM use a lasso penalty while our N-DNA use a hub penalty. A comparison with them would show the gain of the new method due to the consideration of the hub structure of the differential network. PNJGL and N-DNA use a same penalty function. PNJGL jointly estimates the condition-specific precision matrices, while N-DNA directly estimates the differential network. A comparison with PNJGL would show the gain of the new method that does not require estimation of the individual precision matrices. We do not compare N-DNA with fused graphical lasso (Danaher et al., 2014) and the method of Zhao et al. (Zhao et al., 2014) since previous studies have shown that D-trace loss estimate, LDGM and PNJGL outperform the two approaches (Mohan et al., 2014; Tian et al., 2016; Yuan et al., 2015a).

Fig. 2 displays the average performance of the compared approaches over 100 random generations of the data. Each colored line corresponds to the results obtained using a fixed value of the tuning parameter λ_2 , as the tuning parameter λ_1 is varied. Note that D-trace loss estimate and LDGM have one parameter, thus there is only one line for the two approaches. We observe that N-DNA outperforms PNJGL for a suitable range of parameter λ_2 . This result indicates that direct estimation of the differential network works better than method that estimates the individual condition-specific networks, which is in agreement with previous observations (Zhao et al., 2014; Yuan et al., 2015a; Tian et al., 2016). D-trace loss estimate and LDGM perform not as well as N-DNA and PNJGL since the former two methods do not consider the hub structure of the differential network.

We also compare the computational time of each approach (Fig. 3). The complexity of all the three algorithms is $O(p^3)$, which is the complexity of computing the eigenvalue decomposition for D-Trace, PNJGL and N-DNA (Mohan et al., 2014; Yuan et al., 2015a), and the complexity of computing gradient for LDGM (Tian et al., 2016). In (6), the term $(\hat{\Sigma}_X \hat{\Sigma}_Y + \hat{\Sigma}_Y \hat{\Sigma}_X) / 2 + \rho I$, for which we need to compute eigenvalue decomposition, does not require to update in each iteration of the ADMM algorithm. Therefore, we only need to compute the eigenvalue decomposition one time. This is same to D-trace loss estimate (Yuan et al., 2015a). However, PNJGL needs to compute the eigenvalue decomposition two times in each iteration. Therefore, it computes the eigenvalue decomposition $2T$ times in total, where T is the number of iterations. LDGM does not need

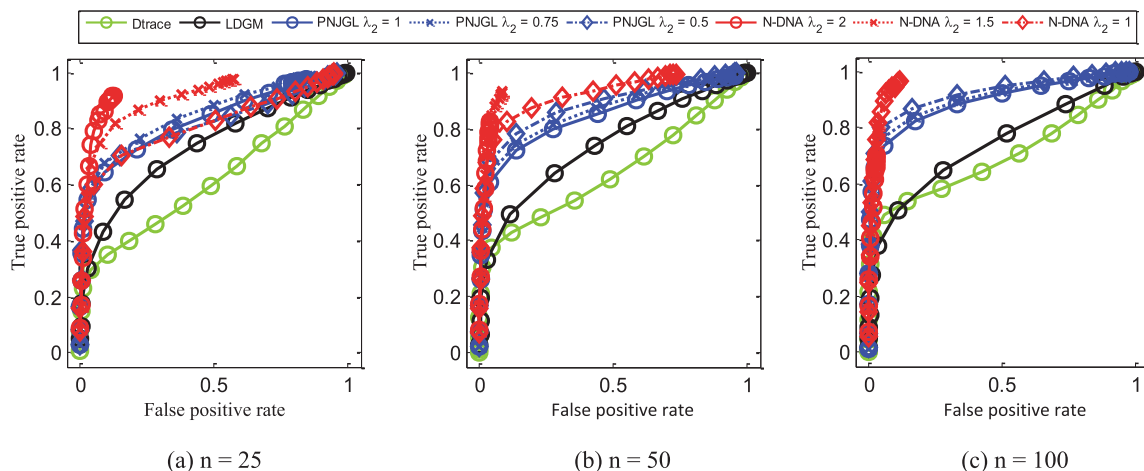


Fig. 2. Receiver operating characteristic curves for support recovery of the true differential network on simulated data. In each panel, the x-axis denotes the false positive rate, and the y-axis denotes the true positive rate. Each colored line corresponds to a fixed value of λ_2 , as λ_1 is varied. Results are averaged over 100 random generations of the data. (a) $n=25$, (b) $n=50$, (c) $n=100$.

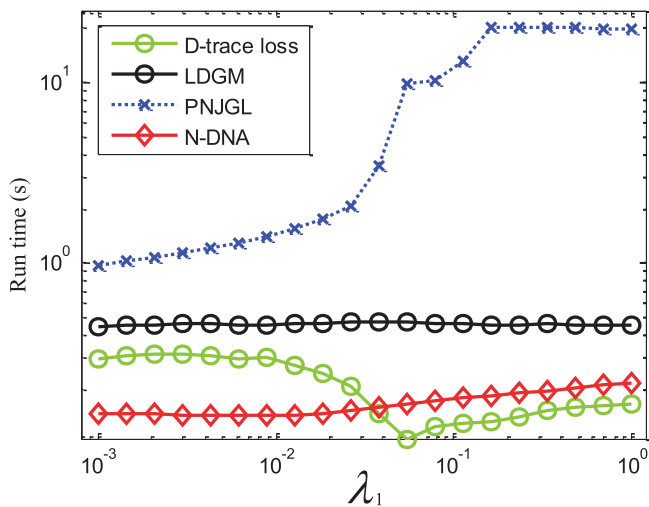


Fig. 3. Run time (in seconds) as a function of λ_1 , with $p = 100$. The x-axis denotes the value of λ_1 , and the y-axis denotes the run time. The two axes are in logarithmic scale. Results are averaged over 100 random generations of the data.

to compute the eigenvalue decomposition but requires to compute the gradient in each iteration. From Fig. 3, we find that N-DNA, LDGM and D-trace loss estimate take only a fraction of computation time of PNJGL. It is also interesting to observe that when λ_1 increases, the time cost of PNJGL increases significantly. This may be partly due to the fact that the number of iterations for the algorithm to terminate increases when λ_1 increases (Mohan et al., 2014). N-DNA, LDGM and D-trace loss estimate are less sensitive to the value of λ_1 since they do not need to compute the eigenvalue decomposition in the iteration process.

3.2. Ovarian cancer application

3.2.1. Data sets

Resistance to platinum-based chemotherapy is the predominant cause of treatment failure and death in ovarian cancer (Bowtell et al., 2015; Holmes, 2015). In this experiment, we aim to identify genes whose interactions with other genes are perturbed significantly between two groups of ovarian tumors with different treatment response (platinum sensitivity and platinum resistance). We apply N-DNA to gene expression data from The Cancer Genome Atlas (TCGA) which are collected from the Affymetrix HT Human Genome U133 Array Plate Set (The Cancer Genome Atlas Research Network, 2011). We download the gene expression profile (level 3) from the TCGA website. As of February 2016, gene expression levels of 12,042 genes for 520 patients are available. Then, a logarithmic transformation is taken to make the data more normally distributed.

We define platinum-based chemotherapy response groups following the method of (Nabavi et al., 2016). Tumors are defined as platinum-sensitive if there is no evidence of disease progression within 6 months of the end of the initial platinum-based treatment, and the follow-up interval is at least 6 months. Tumors which demonstrate recurrence within 6 months following the completion of platinum-based treatment are defined as resistant. Among the 520 patients, 344 patients have explicit platinum status, with 246 platinum sensitive and 98 platinum resistant. All analysis are restricted to the corresponding set of 344 patients. We normalize the expression data to have mean zero and standard deviation one within each group.

We present our analysis of genes that overlap with the mTOR signaling pathway. The mTOR signaling pathway is frequently mutated or altered in ovarian cancer (The Cancer Genome Atlas

Research Network, 2011), and is implicated in resistance to anti-cancer therapies (Burris, 2013; Rodrik-Outmezguine et al., 2016). We download the mTOR signaling pathway from the Kyoto Encyclopedia of Genes and Genomes database (Kanehisa et al., 2010). Out of the 60 genes in the mTOR signaling pathway, 51 genes overlap with our considered gene expression data.

3.2.2. Differential network analysis

We apply N-DNA to the resulting 246×51 and 98×51 gene expression data sets. Since we are interested in identifying hub nodes in the differential network, we fix $\lambda_2 = 1.8$ to obtain a few hub genes. We select λ_1 range from 0.05 to 0.5 using the AIC-type criterion presented in Section 2.4. We run N-DNA with the selected tuning parameters $\lambda_1 = 0.05$ and $\lambda_2 = 1.8$. The estimated differential network is shown in Fig. 4.

Fig. 4 indicates that two hub nodes in differential network are detected: IRS1 and PDKP1. IRS1 plays a key role in transmitting signals from the IGF1 receptors to the PI3K-AKT signalling pathway and the RAS-RAF-MEK-ERK signalling pathway. As a signalling adapter protein, IRS1 can integrate different signalling cascades and has functional role in cancer progression and platinum resistance (Dearth et al., 2007; Eckstein, 2011). Ravikumar et al. (Ravikumar et al., 2007) have revealed that IRS1 is an important mediator of ovarian cancer cell growth suppression and can be a potential effective target for chemotherapeutic intervention. PDKP1, which is a master kinase, is crucial for the activation of the PI3K-AKT signalling pathway. Lohneis et al. (2015) found a negative correlation between PDKP1 expression and ovarian tumor grade, which suggest PDKP1 might be a prognostic marker and a possible therapeutic target in ovarian serous carcinoma. In addition, a recent study showed that PDKP1 is associated with chemoresistance in ovarian cancer cells (Wu et al., 2015).

3.3. Breast cancer application

3.3.1. Data sets

Breast cancer is the leading type of cancer in women worldwide. In this experiment, we focus on identifying key genes that drive changes of gene networks between normal tissue and tumor tissue. We use the TCGA gene expression data which was used by Grechkin et al. (2016). We download the data from <http://discernleelab.cs.washington.edu/>. Gene expression measurements over 10,809 genes for 529 tumor tissues and 61 normal tissues are available. In order to investigate pathway aberrations, we take

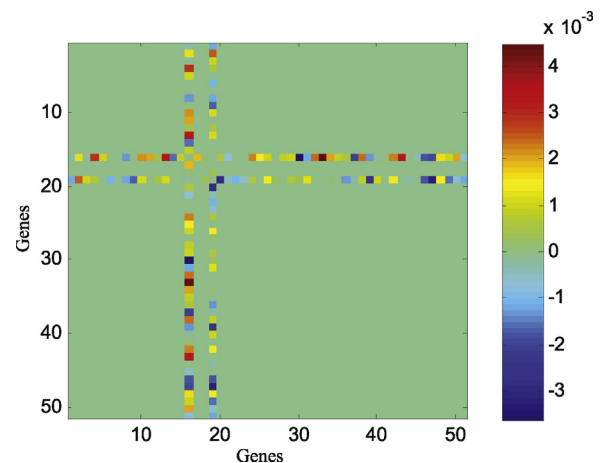


Fig. 4. The differential network estimated by N-DNA between platinum-resistance ovarian tumors and platinum-sensitive ovarian tumors. Only genes contained in the mTOR signaling pathway are considered in the analysis. N-DNA is performed with $\lambda_1 = 0.05$ and $\lambda_2 = 1.8$. Two genes (IRS1 and PDKP1) are identified as hub nodes.

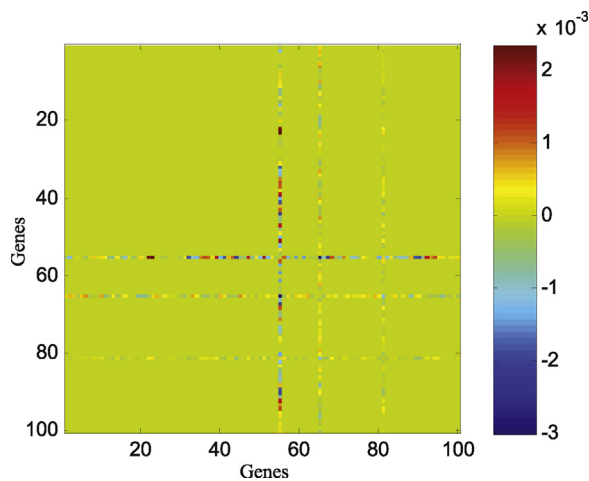


Fig. 5. The differential network estimated by N-DNA between tumor tissue and normal tissue for breast cancer. Only genes contained in the breast cancer pathway are considered. N-DNA is performed with $\lambda_1 = 0.05$ and $\lambda_2 = 7.8$. Three genes (KIT, NOTCH1 and SHC4) are identified as hub nodes.

a pathway-based analysis. We present our analysis of genes that overlap with the breast cancer pathway. We download the breast cancer pathway from the Kyoto Encyclopedia of Genes and Genomes database (Kanehisa et al., 2010). Among the 146 genes in the breast cancer pathway, there are 100 genes in the considered gene expression profiles.

3.3.2. Differential network analysis

N-DNA is applied to the resulting 529×100 and 61×100 gene expression profiles. In order to obtain a few hub nodes, we fix $\lambda_2 = 7.8$. Tuning parameter λ_1 is selected from 0.05 to 0.5 using the AIC-type criterion presented in Section 2.4. In this experiment, we run N-DNA with the selected tuning parameters $\lambda_1 = 0.05$ and $\lambda_2 = 7.8$. The estimated differential network between tumor tissue and normal tissue is presented in Fig. 5.

As can be seen from Fig. 5, there are three key hub nodes in the estimated differential network: KIT, NOTCH1 and SHC4. KIT, also known as CD117, is a type III receptor tyrosine kinase operating in cell signal transduction (Miettinen and Lasota, 2005). When KIT binds to stem cell factor, it forms a dimer that activates its intrinsic tyrosine kinase activity, and in turn phosphorylates and activates signal transduction molecules that propagate the signal in the cell. KIT expression is significantly associated with high tumor grade breast cancers (Simon et al., 2004). KIT mutations often occur in numerous solid and haematological malignancies, and KIT receptor tyrosine kinase is a well-known therapeutic target in human cancers (Roberts and Govender, 2015). NOTCH1 encodes a member of the NOTCH family of proteins that are ligand-dependent transmembrane receptors. Notch protein has been identified on the surface of cancer stem cells and can promote tumor growth and survival. Mutations in NOTCH1 are associated with many human diseases (Garg et al., 2005), and expression of Notch1 correlates with breast cancer progression and prognosis (Yuan et al., 2015c). Notch signaling has emerged as a therapeutic target in breast cancer (Al-Hussaini et al., 2011; Yuan et al., 2015b). MK-0752, which inhibits the Notch signaling pathway, has given promising results in breast cancer treatment. SHC4 is a member of Shc family adapter proteins which are identified as proto-oncogene involved in growth factor signaling (Ravichandran, 2001). SHC4 has been reported to be associated with male reproductive organ cancer. SHC4 plays a critical role in migration of metastatic melanomas and is associated with spontaneous breast cancer development (Gutsche et al., 2016).

In addition, an important paralog of SHC4, SHC1, is a prognostic marker when targeting cancer treatment.

4. Discussion and conclusion

In this work, a new method is developed to estimate the differential network that contains hub nodes. Simulation studies show the competitive performance of our method in terms of both accuracy and efficiency. In real data analysis, we detect two hub nodes in the differential network associated with platinum response in ovarian cancer, and three hub nodes in the differential network between tumor tissue and normal tissue in breast cancer. According to literature analysis, we find the five hub genes play an important role in ovarian cancer and breast cancer. These results show that N-DNA is a powerful tool for differential network analysis in genomics.

It is computationally prohibitive for Gaussian graphical model-based methods to scale up (Grechkin et al., 2015). This is because most of algorithms that are used to solve the models require to compute the eigendecomposition of a $p \times p$ matrix, where p is the number of genes. Even though our algorithm needs to compute the eigendecomposition only once, the time cost is also $O(p^3)$. When p is very large, it will be computationally very expensive. In this work, we take a pathway-based analysis to handle this problem. In order to analyze genome-wide data, we need to improve the algorithmic efficiency by considering the pathway-based constraints in the future following the idea of pathway graphical lasso (Grechkin et al., 2015).

A common challenge in evaluating the performance of differential network analysis methods using real data is the lack of the gold standard (Tian et al., 2016). In other words, in our cancer data analysis, we cannot obtain condition-specific gene networks and therefore do not have the reference set of differential networks. Therefore, it is difficult to compare different methods in terms of the accuracy of the estimated differential networks. As a result, we only compare our methods with state-of-the-art methods using simulated data and apply our method to real data to explore new biological knowledge.

Our study may be extended in the following aspects. N-DNA assumes the data arise from a Gaussian distribution. This assumption only holds for microarray-based gene expression data and is violated for data from sequencing technologies. Thus, our model is limited to gene expression data from microarrays. It is of interest to extend N-DNA to model non-Gaussian data. In addition, we will consider applying our model to other machine learning algorithms which require the computation of the difference between two precision matrices (e.g., quadratic discriminant analysis (Jiang et al., 2015)).

Acknowledgements

This work was supported by the National Science Foundation of China [grant numbers 61402190, 61532008 and 61602309], Self-determined Research Funds of CCNU from the colleges' basic research and operation of MOE [grant numbers CCNU15A05039 and CCNU15ZD011], and HongKong Research Grants Council [grant numbers C1007-15G].

References

- Al-Hussaini, H., Subramanyam, D., Reedijk, M., Sridhar, S.S., 2011. Notch signaling pathway as a therapeutic target in breast cancer. *Mol. Cancer Therapeut.* 10 (1), 9–15.
- Barabási, A.-L., Gulbahce, N., Loscalzo, J., 2011. Network medicine: a network-based approach to human disease. *Nat. Rev. Genet.* 12 (1), 56–68.
- Bowtell, D.D., et al., 2015. Rethinking ovarian cancer ii: reducing mortality from high-grade serous ovarian cancer. *Nat. Rev. Cancer* 15 (11), 668–679.

- Boyd, S., Parikh, N., Chu, E., Peleato, B., Eckstein, J., 2011. Distributed optimization and statistical learning via the alternating direction method of multipliers. *Foundations Trends® Mach. Learn.* 3 (1), 1–122.
- Burris III, H.A., 2013. Overcoming acquired resistance to anticancer therapy: focus on the pi3k/akt/mTOR pathway. *Cancer Chemother. Pharmacol.* 71 (4), 829–842.
- Cox, D.R., Wermuth, N., 1996. *Multivariate Dependencies: Models, Analysis and Interpretation*. Vol. 67. CRC Press, Boca Raton.
- Danaher, P., Wang, P., Witten, D.M., 2014. The joint graphical lasso for inverse covariance estimation across multiple classes. *J. Royal Stat. Soc.: Series B (Stat. Methodol.)* 76 (2), 373–397.
- de la Fuente, A., 2010. From 'differential expression' to 'differential networking'-identification of dysfunctional regulatory networks in diseases. *Trends Genet.* 26 (7), 326–333.
- Dearth, R.K., Cui, X., Kim, H.-J., Hadsell, D.L., Lee, A.V., 2007. Oncogenic transformation by the signaling adaptor proteins insulin receptor substrate (irs)-1 and irs-2. *Cell Cycle* 6 (6), 705–713.
- Eckstein, N., 2011. Platinum resistance in breast and ovarian cancer cell lines. *J. Exp. Clin. Cancer Res.* 30 (1), 1.
- Friedman, J., Hastie, T., Tibshirani, R., 2008. Sparse inverse covariance estimation with the graphical lasso. *Biostatistics* 9 (3), 432–441.
- Friedman, J., Hastie, T., Tibshirani, R., 2010. A note on the group lasso and a sparse group lasso. *arXiv preprint arXiv:1001.0736*.
- Friedman, N., 2004. Inferring cellular networks using probabilistic graphical models. *Science* 303 (5659), 799–805.
- Garg, V., Muth, A.N., Ransom, J.F., Schluterman, M.K., Barnes, R., King, I.N., Grossfeld, P.D., Srivastava, D., 2005. Mutations in notch1 cause aortic valve disease. *Nature* 437 (7056), 270–274.
- Gill, R., Datta, S., Datta, S., 2010. A statistical framework for differential network analysis from microarray data. *BMC Bioinformatics* 11 (1), 95.
- Grechkin, M., Fazel, M., Witten, D., Lee, S.-I., 2015. Pathway graphical lasso. In: *Proceedings of the AAAI Conference on Artificial Intelligence*. Vol. 2015. NIH Public Access, p. p2617.
- Grechkin, M., Logsdon, B.A., Gentles, A.J., Lee, S.-I., 2016. Identifying network perturbation in cancer. *PLoS Comput. Biol.* 12 (5), e1004888.
- Guo, J., Levina, E., Michailidis, G., Zhu, J., 2011. Joint estimation of multiple graphical models. *Biometrika* 98 (1), 1–15.
- Gutsche, K., Randi, E., Blank, V., Fink, D., Wenger, R.H., Leo, C., Scholz, C.C., 2016. Intermittent hypoxia confers pro-metastatic gene expression selectively through NF- κ B in inflammatory breast cancer cells. *Free Rad. Biol. Med.*
- Ha, M.J., Baladandayuthapani, V., Do, K.-A., 2015. Dingo: differential network analysis in genomics. *Bioinformatics* 31 (21), 3413–3420.
- Holmes, D., 2015. Ovarian cancer: beyond resistance. *Nature* 527 (7579), S217–S217.
- Huang, F., Chen, S., 2015. Joint learning of multiple sparse matrix Gaussian graphical models. *IEEE Trans. Neural Netw. Learn. Syst.* 26 (11), 2606–2620.
- Ideker, T., Krogan, N.J., 2012. Differential network biology. *Mol. Syst. Biol.* 8 (1), 565.
- Jiang, B., Wang, X., Leng, C., 2015. Quda: A direct approach for sparse quadratic discriminant analysis. *arXiv preprint arXiv:1510.00084*.
- Kanehisa, M., Goto, S., Furumichi, M., Tanabe, M., Hirakawa, M., 2010. Kegg for representation and analysis of molecular networks involving diseases and drugs. *Nucl. Acids Res.* 38 (suppl 1), D355–D360.
- Lauritzen, S.L., 1996. *Graphical Models*. Oxford Press, Oxford.
- Lee, W., Liu, Y., 2015. Joint estimation of multiple precision matrices with common structures. *J. Mach. Learn. Res.* 16, 1035–1062.
- Lin, Z., Chen, M., Ma, Y., 2010. The augmented lagrange multiplier method for exact recovery of corrupted low-rank matrices. *arXiv preprint arXiv:1009.5055*.
- Lohneis, P., Darb-Esfahani, S., Dietel, M., Braicu, I., Sehouli, J., Arsenic, R., 2015. Pdk1 is expressed in ovarian serous carcinoma and correlates with improved survival in high-grade tumors. *Anticancer Res.* 35 (11), 6329–6334.
- Markowitz, F., Spang, R., 2007. Inferring cellular networks—a review. *BMC Bioinformatics* 8 (Suppl 6), S5.
- Miettinen, M., Lasota, J., 2005. Kit (cd117): a review on expression in normal and neoplastic tissues, and mutations and their clinicopathologic correlation. *Appl. Immunohistochem. Mol. Morphol.* 13 (3), 205–220.
- Mohan, K., London, P., Fazel, M., Witten, D.M., Lee, S.-I., 2014. Node-based learning of multiple Gaussian graphical models. *J. Mach. Learn. Res.* 15 (1), 445–488.
- Nabavi, S., Schmolze, D., Maitituoheti, M., Malladi, S., Beck, A.H., 2016. Emdomics: a robust and powerful method for the identification of genes differentially expressed between heterogeneous classes. *Bioinformatics* 32 (4), 533–541.
- Ou-Yang, L., Dai, D.Q., Li, X.L., Wu, M., Zhang, X.F., Yang, P., 2014. Detecting temporal protein complexes from dynamic protein-protein interaction networks. *BMC Bioinformatics* 15 (1), 335.
- Parikh, N., Boyd, S., 2014. Proximal algorithms. *Foundations Trends® Optimiz.* 1 (3), 127–239.
- Peng, J., Wang, P., Zhou, N., Zhu, J., 2012. Partial correlation estimation by joint sparse regression models. *J. Am. Stat. Assoc.* 104 (486), 735–746.
- Ravichandran, K.S., 2001. Signaling via shc family adapter proteins. *Oncogene* 20 (47), 6322–6330.
- Ravikumar, S., Perez-Liz, G., Del Vale, L., Soprano, D.R., Soprano, K.J., 2007. Insulin receptor substrate-1 is an important mediator of ovarian cancer cell growth suppression by all-trans retinoic acid. *Cancer Res.* 67 (19), 9266–9275.
- Roberts, R., Govender, D., 2015. Gene of the month: Kit. *J. Clin. Pathol.* 68 (9), 671–674.
- Rodrik-Outmezguine, V.S., et al., 2016. Overcoming mTOR resistance mutations with a new-generation mTOR inhibitor. *Nature* 534 (7606), 272–276.
- Rothman, A.J., Bickel, P.J., Levina, E., Zhu, J., 2008. Sparse permutation invariant covariance estimation. *Electr. J. Stat.* 2, 494–515.
- Simon, R., Panussis, S., Maurer, R., Spichtin, H., Glatz, K., Tapia, C., Mirlacher, M., Ruffe, A., Thorhorst, J., Sauter, G., 2004. Kit (cd117)-positive breast cancers are infrequent and lack kit gene mutations. *Clin. Cancer Res.* 10 (1), 178–183.
- Tan, K.M., London, P., Mohan, K., Lee, S.-I., Fazel, M., Witten, D.M., 2014. Learning graphical models with hubs. *J. Mach. Learn. Res.* 15 (1), 3297–3331.
- The Cancer Genome Atlas Research Network, 2011. Integrated genomic analyses of ovarian carcinoma. *Nature* 474 (7353), 609–615.
- Tian, D., Gu, Q., Ma, J., 2016. Identifying gene regulatory network rewiring using latent differential graphical models. *Nucl. Acids Res.* 44 (17), e140–e140.
- Wu, Y.-H., Chang, T.-H., Huang, Y.-F., Chen, C.-C., Chou, C.-Y., 2015. Col11a1 confers chemoresistance on ovarian cancer cells through the activation of akt/c/ebp β pathway and pdk1 stabilization. *Oncotarget* 6 (27), 23748–23763.
- Yuan, H., Xi, R., Deng, M., 2015a. Differential network analysis via the lasso penalized d-trace loss. *arXiv preprint arXiv:1511.09188*.
- Yuan, M., Lin, Y., 2007. Model selection and estimation in the gaussian graphical model. *Biometrika* 94 (1), 19–35.
- Yuan, X., Wu, H., Xu, H., Xiong, H., Chu, Q., Yu, S., Wu, G.S., Wu, K., 2015b. Notch signaling: an emerging therapeutic target for cancer treatment. *Cancer Lett.* 369 (1), 20–27.
- Yuan, X., Zhang, M., Wu, H., Xu, H., Han, N., Chu, Q., Yu, S., Chen, Y., Wu, K., 2015c. Expression of notch1 correlates with breast cancer progression and prognosis. *PLoS ONE* 10 (6), e0131689.
- Zhang, T., Zou, H., 2014. Sparse precision matrix estimation via lasso penalized d-trace loss. *Biometrika* (1), 103–120.
- Zhang, X.F., Ou-Yang, L., Dai, D.Q., Wu, M.Y., Zhu, Y., Yan, H., 2016a. Comparative analysis of housekeeping and tissue-specific driver nodes in human protein interaction networks. *BMC Bioinformatics* 17 (1), 358.
- Zhang, X.F., Ou-Yang, L., Hu, X., Dai, D.Q., 2015a. Identifying binary protein-protein interactions from affinity purification mass spectrometry data. *BMC Genomics* 16 (1), 745.
- Zhang, X.F., Ou-Yang, L., Zhao, X.M., Yan, H., 2016b. Differential network analysis from cross-platform gene expression data. *Sci. Rep.* 6 (1), 34112.
- Zhang, X.F., Ou-Yang, L., Zhu, Y., Wu, M.Y., Dai, D.Q., 2015b. Determining minimum set of driver nodes in protein-protein interaction networks. *BMC Bioinformatics* 16 (1), 146.
- Zhao, S.D., Cai, T.T., Li, H., 2014. Direct estimation of differential networks. *Biometrika* 101 (2), 253–268.